

FLOW CHARACTERISTICS OF TWO-DIMENSIONAL JET IN CROSS FLOW

خصائص السريان لمنفوث ثنائي الأبعاد في تيار متعارض

S. H. El-Emam*, H. Mansour*, A. R. Abdel-Rahim*, and M. M. El-Khayat**

*Faculty of Engineering, Mansoura University, Mansoura, Egypt.

** NREA, P.O.Box 4544 Masakin Dobat El-Saff, El-Hay El-Sades, Nasr city, Cairo, Egypt

ملخص البحث

يشتمل البحث على دراسة نظرية وتجريبية لتحليل خصائص المنفوثات ثنائية الأبعاد في تيار متعارض بهدف التوصل إلى إيجاد علاقة بين مسارات المنفوثات التي يتم تتبعها تجريبياً بدلالة نسبة التركيز وتلك التي يتم استنتاجها نظرياً بناءً على سرعة السريان، وذلك بمقارنة النتائج التجريبية لمنفوث - صادر من شق بعرض 1 مم- في تيار متعارض مع نتائج نموذج رياضي ثنائي الأبعاد. وقد لجرى الدراسة عند نسب سرعات مختلفة بين المنفوث والتيار المتعارض. كما تم إعداد برنامج يمكن من خلاله تحليل ودراسة نتائج التجارب واعتباره جزءاً مكملاً لتقنية "رقمنة الصور" والتي استخدمت في هذا البحث. وتشير النتائج إلى وجود توافق مرضي لمسار المنفوث في كل من حالتي الاستناد على نسب التركيز التجريبية وسرعة السريان النظرية للمنفوث. وبناءً على ذلك فإنه من الممكن تعميم ذلك في حالة دراسة المنفوثات ثلاثية الأبعاد. كما تم أيضاً استنتاج معادلة تجريبية لتتبع مسارات المنفوثات ثنائية الأبعاد كدالة في قطر الرشاش ونسبة السرعة بين المنفوث والتيار المتعارض، وهذه المعادلة صالحة لتحديد مسار المنفوث في كل من المنطقة القريبة و البعيدة من فوهة الرشاش في أن واحد.

Abstract

To study the flow characteristics of a two-dimensional jet in crossflow, a slit jet of 1 mm width has been used. The concentration distribution was obtained experimentally using image digitizing technique. The velocity distribution was theoretically studied using a two-dimensional model. A jet centerline trajectory was traced based on both maximum concentration values and maximum velocity values along the flow field for the experimental and theoretical cases, respectively. A reasonable agreement was indicated between both traces. This result can be extended for studying the three-dimensional jets in crossflow. An experimental correlation has been developed for jets in crossflow at different velocity ratios for both near – and far-field.

Nomenclature

A	empirical dimensionless constant, Eq.(4)	U	x-direction velocity component, m/s
B	empirical dimensionless constant, Eq.(4)	U_∞	crossflow velocity, m/s
C	empirical dimensionless constant, Eq.(4)	W_j	slit jet width
CAST	computer-aided simulation turbulence	V_R	velocity ratio, jet velocity to crossflow velocity
CVPs	counter-rotating vortex pairs	\bar{X}	dimensionless horizontal Cartesian coordinates
D	empirical dimensionless constant, Eq.(4)	\bar{Y}	dimensionless vertical Cartesian coordinates
JICF	jet in crossflow	ρ_j	jet flow density, kg/m ³
P	pressure, N/m ²	U_j	jet flow velocity, m/s
S	distance along the centerline trajectory, m	ρ_∞	crossflow density, kg/m ³

1. Introduction

It is known that when a jet discharges into a crossflow, a complicated interaction between the two flows is happened. The jet enters into the crossflow and then bends over in the stream wise direction until the jet flow is aligned with the crossflow. Therefore, the flow field generated by a jet in crossflow, JICF, is very complex, unsteady, and highly turbulent. The JICF has been found in a wide variety of practical applications, such as primary combustion zones in gas turbine combustors, over-fire cooling systems, chimneys exhaust plumes and many other industrial applications.

Roth (1988) has mentioned that, a jet exhausting perpendicularly into a crossflow deflects, increases in lateral extent, distorts in cross sectional shape and evolves into a flow field that is dominated by a pair of counter-rotating vortex, CVPs.

Krothapalli *et al* (1981), Raman and Taghavi (1996), Smith and Mungal (1998), and Hasselbrink (1999) divided the flow obtained from a JICF into three regions; the potential core region, in the first few diameters from the jet exit; the near-field region, just beyond the potential core, where the flow is fully turbulent but has not deflected appreciably, and the far-field region, where the jet's flow has turned almost completely into the crossflow. In addition, they mentioned that, the first region is similar

to an axi-symmetric mixing layer, the second region, is similar to a free jet, and the third region, is similar to a wake.

In order to clarify the interaction between both crossflow and the jet flow, it is important to define the velocity ratio. There are two definitions considered; the first definition of the velocity ratio is defined by Andreopoulos (1985), Smith (1996), and Smith and Mungal (1998), as the ratio between jet momentum to the crossflow momentum. This definition is recommended in case of studying JICF with different densities. On the other hand Gosh and Hunt (1998) had used the inverse of this definition. The second definition was introduced by Roth (1988), and Kelso *et al* (1996), as the ratio of the jet velocity to the free stream velocity, for the same fluid of jet and crossflow, also they recommended this definition for subsonic and unheated jets. In this study, the second definition has been considered. As mentioned by Abdel-Rahim *et al* (2003), the determination of the jet trajectory is defined to be the locii of points of maximum concentration in the direction of the jet within the flow symmetry path.

In the absence of a crossflow the centerline temperature for a vertical jet discharged into a uniform ambient temperature has been discussed by Ogino *et al* (1980). They mentioned that, if a heated jet discharged into a stable stratified environment, the mixing of the jet fluid and the ambient fluid makes the jet denser and eventually the buoyancy force acting on the jet. Then the jet will stop rising when the upward momentum vanishes by the action of buoyancy force. Thus the jet will spread horizontally in a thin layer.

Abramovich (1963), Beer and Chigier (1974), and Schetz (1980) reviewed several publications concerning JICF and they concluded that, the flow field of the JICF depends primarily upon the velocity ratio. They also, mentioned that velocity measurements along the centerline plan of the jet, and at perpendicular sections are Gaussian shaped. Meanwhile, concentration distributions at different cross sections have been studied using many authors e.g. Smith (1996), Smith and Mungal (1998), and Hasselbrink (1999). They reported that concentration distributions have either the top-hat shape, or the two-level distributions.

The two-dimensional motion of a cylinder of fluid released into a crossflow that is uniform far upstream of the cylinder was studied by Rottman *et al* (1987). The cylinder has been considered containing the fluid at rest to be circular. The results of the numerical calculations show that the circular cross section of the released fluid first deforms either for inviscid or viscous flows.

From the previous survey it can be concluded that both concentration distribution and velocity distribution were studied separately. Therefore the main objective of this study is to find the relation between both velocity and concentration distributions for the two-dimensional JICF. In addition, develop a two-dimensional empirical formula to predict jet centerline trajectory for JICF systems.

2. Theoretical Analysis

In this study the model titled computer aided simulation of turbulent, CAST, developed by Milovan and Scheurer (1989) has been adopted to simulate the two-dimensional JICF. CAST is similar in structure to the existing fluid flow prediction procedures, but it differs from those code in the co-located variable arrangement, the discretization scheme, the solution algorithms for the linear equation systems arising from discretization, and in the pressure velocity coupling.

The Reynolds-averaged Navier-Stokes equations of motion for two-dimensional turbulent in Cartesian coordinates are;

Conservation of mass;

$$\frac{\partial(\rho U)}{\partial x} + \frac{\partial(\rho V)}{\partial y} = 0 \quad (1)$$

Conservation momentum in X-direction;

$$\frac{\partial}{\partial x} (\rho U^2 + \overline{\rho u^2}) + \frac{\partial}{\partial y} (\rho UV + \overline{\rho uv}) = - \frac{\partial P}{\partial x} \quad (2)$$

Conservation momentum in Y-direction;

$$\frac{\partial}{\partial x} (\rho UV + \overline{\rho uv}) + \frac{\partial}{\partial y} (\rho V^2 + \overline{\rho v^2}) = - \frac{\partial P}{\partial y} \quad (3)$$

In this model turbulent flows and the fluid properties have been interpreted as time, or ensemble-averaged, averages are indicated by over bars. The viscous terms in the momentum equations are neglected assuming high Reynolds numbers. The correlations $-\rho \overline{u^2}$, $-\rho \overline{uv}$, and $-\rho \overline{v^2}$ represent the transport of momentum by the turbulent fluctuating motion. They act like stresses on fluid elements and are therefore called Reynolds stresses. These stresses are additional unknowns in the equation set (1) to (3) and must be related to known quantities via a turbulence model to enable a closed solution of the flow equations.

The K- ϵ turbulence model presented by Launder and Spalding (1974), is employed in CAST, makes use of the eddy viscosity hypothesis setting the Reynolds stresses proportional to the mean strain rates. Numerical solution procedure based on the flow equations presented here is solved with a conservative finite-volume method, Patankar (1980). Figure (1) displays the computational domain used to simulate the two-dimensional experimental system.

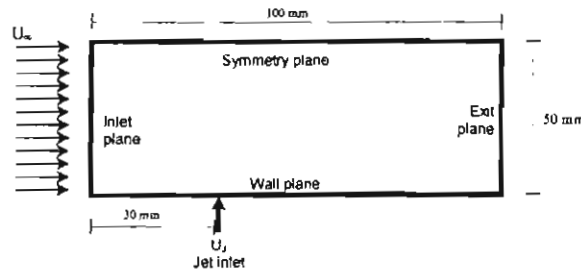


Fig.(1): Computational domain used to simulate the experimental system

3. Experimental Set Up

An arrangement of the experimental test rig is shown in Fig. (2). A Plexiglas 1' x 1' square cross section of 2' length mounted in a sub-sonic wind tunnel is used as a test section to study the concentration variation at different cross sections in both near- and far-field. Slit jet is mounted at the inlet plane of the test section, and is fitted with a heat exchanger to reduce temperature of the paraffin smoke produced from a smoke generator to the ambient temperature. In addition, a sheet of light with 0.25 mm in width is produced from a lighting source aligned to the center of the jet and parallel to the free stream, and images are captured using a high-speed camera. The test section is painted with a black color to avoid external light reflection. Pressure and temperature of the smoke have been measured by digital micro-manometer, and digital non-contact thermometer, respectively. Meanwhile a digital illuminance meter has been used to check darkness of the test section. A slit jet of 200mm x 1mm is mounted between the bell-mouth entrance of the wind tunnel and the test section. For mounting purpose the metallic test section flange hides a length of 20 mm from the jet center. Used jet velocities are 1, 2, and 2.8 m/s, and crossflow velocity is fixed at 1m/s. The experimental records have been analyzed using image digitizing technique presented by El-Khayat (2002). This technique is based on converting image into a group of digits; each digit represents a unique color degree. This digit will be repeated whenever its corresponding color degree exists.

4. Results

Results of studying the two-dimensional jet flows from the slit jet perpendicular to the crossflow are presented here. This has been done to investigate the relation between velocity distributions and concentration distributions. In this study the horizontal distance, X , is measured from the centerline of the slit jet in the crossflow direction, and the vertical distance, Y , is measured from the centerline of the slit jet exit in the jet direction.

Three instantaneous images and their mean image of a two-dimensional JICF at $V_R = 2.8$ are shown in Fig. (3). One can see that, although the instantaneous images have been taken for the same operating conditions, three main deviations can be observed. The first deviation appears in the concentration distribution; represented as color variation. The second deviation is in the trajectory path and consistency, and the third deviation has been occurred in the jet deformation. Consequently, any of them can't be considered as a successful representation for this case, and the mean image must be derived. For the same case study 15 sequential images were taken, the time interval between two sequential images is 6 seconds, and their mean image has been produced using FLUIDLAB package presented by Abdel-Rahim *et al* (2003).

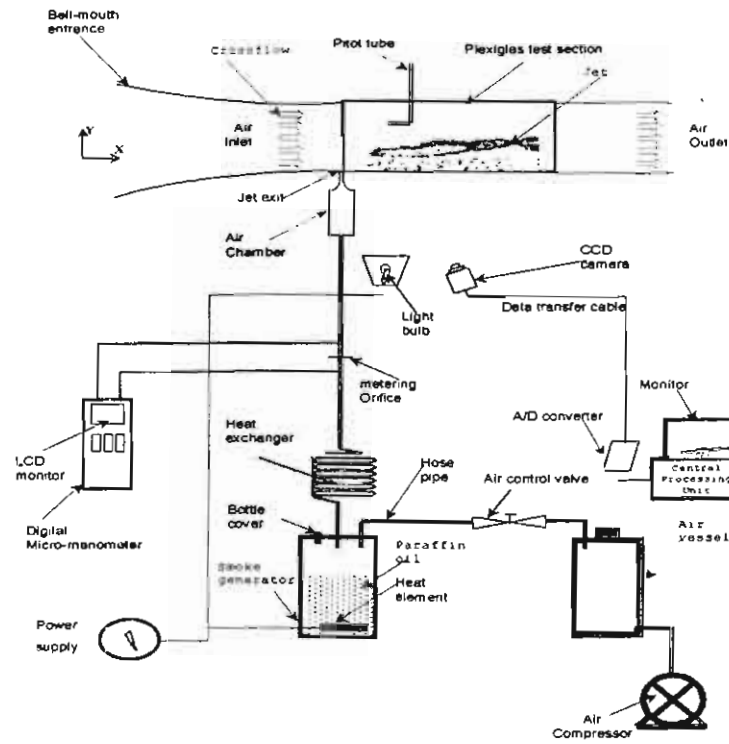


Fig. (2): Schematic of the experimental rig arrangement

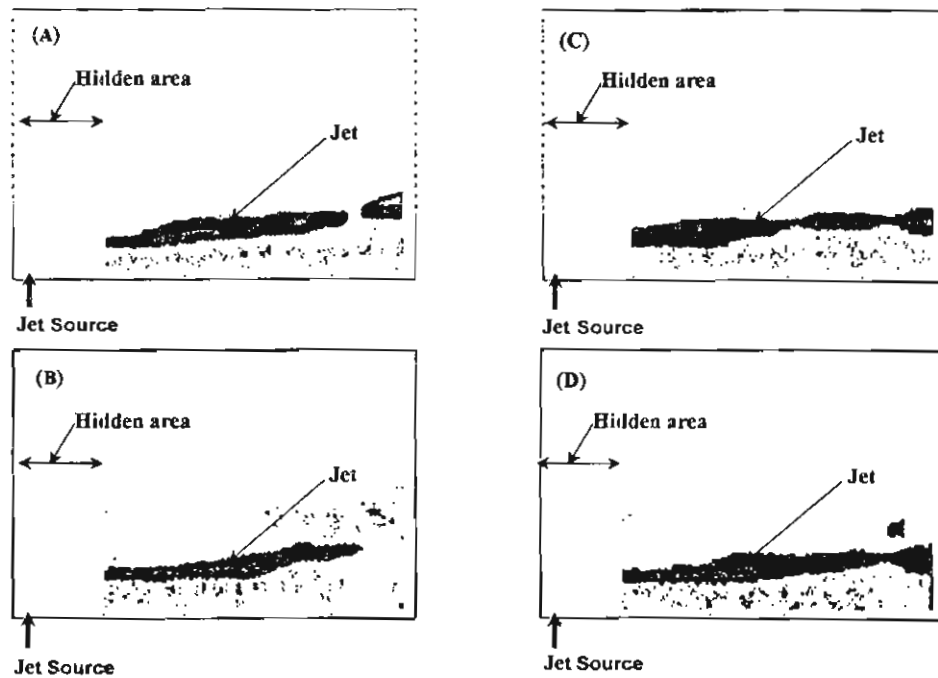


Fig.(3): Three instantaneous images (A), (B), and (C) of the JICF, and their mean image (D). (Slit jet of 200mm x 1mm, $V_R=2.8$)

4.1 Velocity and concentration distributions

CAST model has been used to obtain streamline patterns for JICF velocity ratios of 1.0, 2.0, and 2.8 as shown in Fig. (4). In this Figure X and Y axis are in dimensionless form relative to the jet width, W_j . Also, predicted velocity distributions of a two-dimensional JICF at different velocity ratios are shown in Fig. (5). The influence of the crossflow on the jet flow is clearly shown at velocity ratio 1.0, where crossflow suppress the jet flow. On the other hand, far from the jet exit, streamline patterns tend to take the direction of the crossflow. Also, it can be seen that there is a recirculation zone located underneath the jet. This may be due to the fact that jet works as a separator between both crossflow and the wake region. This hypothesis has been visually noticed through the experimental record measurements, and confirmed by the obtained velocity distribution. Each case in Fig. (5) has been scaled relative to the crossflow vector length.

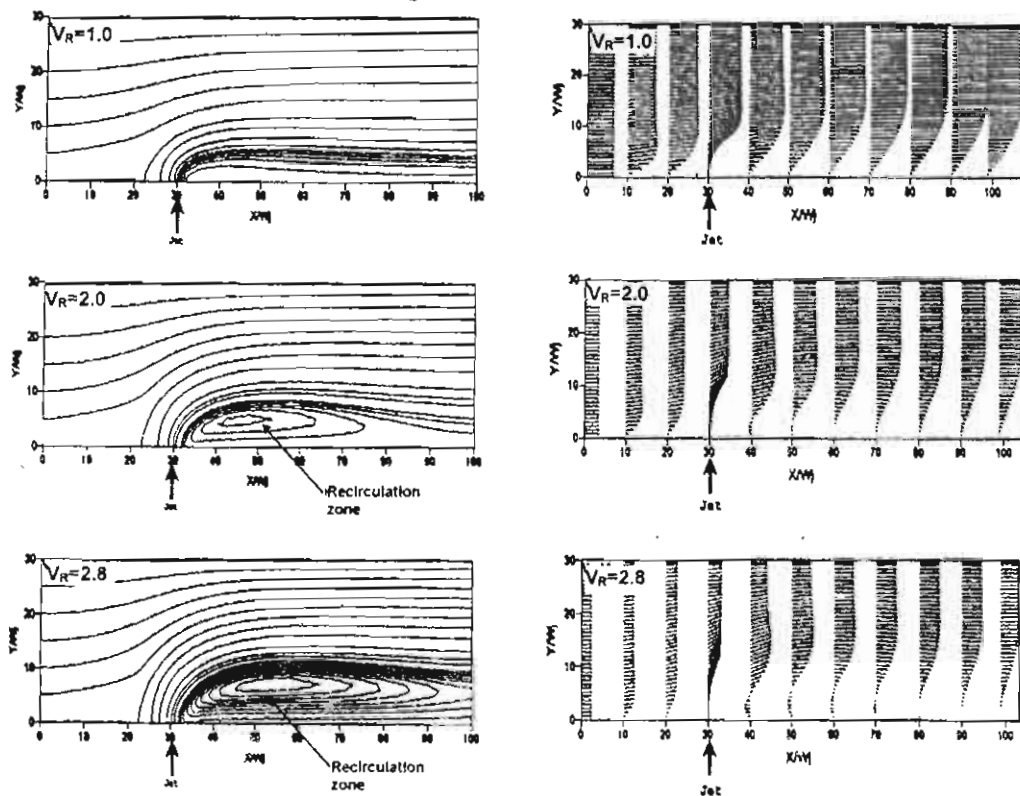


Fig.(4): Streamline patterns for a JICF. Slit jet of 1mm in width, for different velocity ratios

Fig.(5): Velocity distribution for a JICF. Slit jet of 1mm in width, for different velocity ratios

On the other hand, FLUIDLAB package, presented by Abdel-Rahim et al (2003), has been used to produce jet profiles as well as concentration profiles from the experimental results done for the same velocity ratios of the two-dimensional JICF. Samples of these results: at $V_R = 2.0$, and 2.8 have been presented in Fig.(6). It is clearly shown that jet characteristics are related to the velocity ratio. Also, the extrapolated data are represented by dashes started from the origin of the jet to horizontal length of 20 cm.

In addition, the real data for concentration profiles, where concentration is normalized by concentration at the jet exit, is characterized by sharp gradients and nearly can be considered as Gaussian shaped profiles. Also, it can be noticed that the mixed fluid compositions across the entire jet are within a narrow range of concentrations relative to the mean profile, so they can be classified as "top-hat" type, such as those illustrated by Dahm and Dimotakis (1987). These profiles are averaged

by a smooth Gaussian profiles and presented in Fig. (7). It can be mentioned that concentration distribution tends to be weak with increasing X/W_j .

4.2 Jet centerline

The maximum values of the jet concentration along the centerline plane of the jet are available from the side-view images. From the locii positions of the maximum values of the concentration the trajectory of the jet centerline can be obtained, this assumption is recommended by Smith (1996), and Hasselbrink (1999). The maximum values itself give the centerline concentration decay in two possible coordinate systems: X, Y, or S. Where S refers to the distance along the centerline trajectory.

From the experimental results, the raw concentration data and the curve fits are obtained. The concentration data are selected by passing a line perpendicular to the jet direction and determining the position of maximum concentration along each line, then the jet trajectory based on concentration distribution can be obtained. On the other hand, CAST model provides velocity distributions for the cases under-discussion. As a result of determining locations of maximum values for both concentration and velocity distributions, jet centerlines can be drawn and matched, as shown in Fig. (8).

It can be stated from Fig. (8) that reasonable agreement between both experimental results (based on maximum concentration distribution), and theoretical results (based on velocity distribution) is nearly occurred at different velocity ratios. The fact that theoretical jet trajectory is higher than the experimental trajectory may be due to the approximations inherent in the CAST model, or the effect of the geometrical configuration which account for the slight difference in the jet centerline. Accordingly, It can be concluded that both jet trajectories can be represented either by locations of maximum velocity or locations of maximum concentration. Based on this result it can be concluded that, the image digitizing technique used in this study can be used to investigate JICF for the three-dimensional case.

For the purpose to obtain a general correlation to detect jet trajectory for the two-dimensional JICF, the concentration data for each velocity ratio is individually fit to the following relationship, which based on velocity ratio, and jet width which

$$\tilde{Y} = A \cdot V_R^B \cdot \frac{\tilde{X} - C}{\tilde{X} + D} \tag{4}$$

The reason of applying this formula backs to, based on visual observations it has been noticed that the jet starts vertically then deflects on a result of the interaction with the crossflow, then takes the

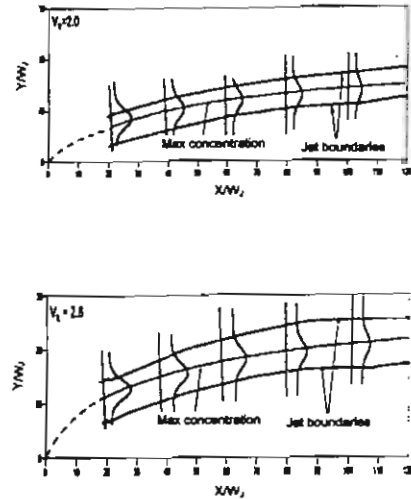


Fig.(6): Experimental jet trajectories, boundaries and dimensionless concentration distribution. Slit jet of 200mm x 1mm, for different velocity ratios

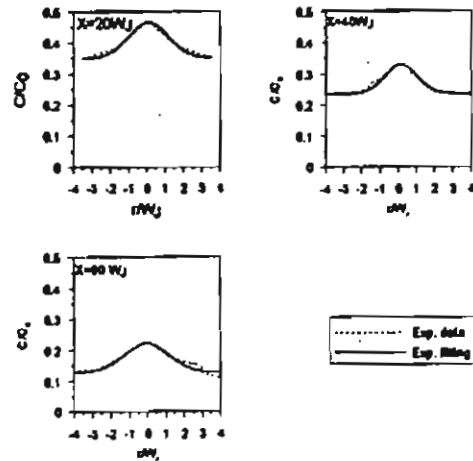


Fig.(7): Ensemble-averaged concentration distribution. Slit jet 200mm x 1mm, $V_R=2.8$.

direction of the crossflow. This trend has been found similar to the trend obtained from the presented equation, which called saturation equation. From the obtained experimental results the values of A, B, C and D were calculated and presented in table (1).

Table(1) The constants A, B, C and D for the two-dimensional JICF

A	B	C	D
20.0	0.25	0.0	28.3

By introducing values presented in table (1) into Eq. (4), a new centerline formula able to trace and predict jet trajectory for a two-dimensional JICF can be obtained. The final equation can be written as follows;

$$\tilde{Y} = 20 * V_R^{0.25} * \frac{\tilde{X}}{\tilde{X} + 28.3} \quad (5)$$

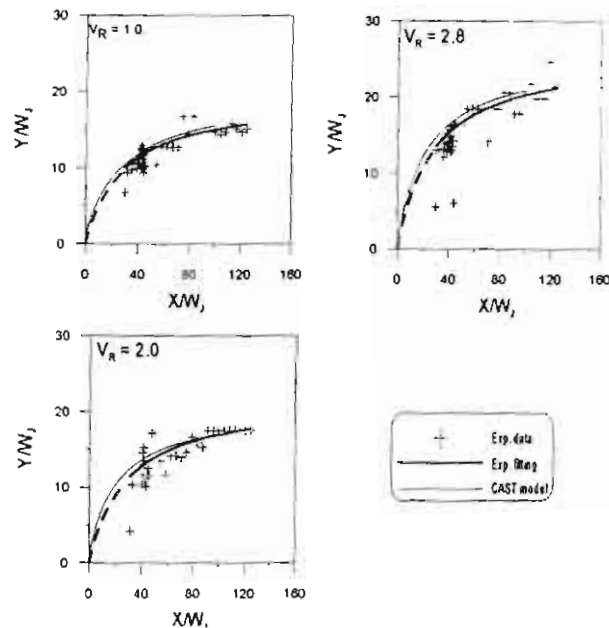


Fig. (8): Experimental, and theoretical jet centerlines. Slit jet of 200 mm x 1 mm, for different velocity ratios.

5) Conclusions

From the obtained results the following conclusions have been reached;

- The two-dimensional study showed that the jet centerline based on the velocity distribution of the computational results, matches with that based on the experimental concentration distribution.
- In the three-dimensional jet studies the velocity distribution could be estimated from the experimental concentration distribution or vice versa, for the present work.
- The obtained correlation for tracing jet centerline for the two-dimensional JICF can be used in both near- and far-field, for the specific studied case.

6) References

- Abdel-Rahim, A.R., Mansour, H., El-Emam, S. H., and El-Khayat, M. M., "Jet characteristics using image digitizing technique," to be published
- Abramovich, G.N. (1963), "The Theory of turbulent jets," Textbook, The Massachusetts Institute of Technology.
- Andreopoulos, J. (1985), "On the structure of jets in a crossflow," *J. of Fluid Mech.*, 157, 163 – 197.
- Beer, J.M. and Chigier, N.A. (1974), "Combustion aerodynamics," Applied science publishers LTD.
- Dahm, W.J.A., and Dimotakis, P.E. (1987), "Measurements of entrainment and mixing in turbulent jets," *AIAA J.*, 25 (9), 1216 – 1223.
- El-Khayat, M. M. (2002), "Study of flow characteristics of jets in crossflow," Ph.D. Thesis, Mansoura University
- Gosh, S. and Hunt, J.C.R. (1998), "Spray jets in crossflow," *J. of Fluid Mech.*, 365, 109 – 136.
- Hasselbrink, E.F. (1999), "Transverse jets and jets flames: structure, scaling, and effects of heat release," Ph.D. thesis, Stanford University.

- Kelso, R.M., Lim, T.T. and Perry, A. E. (1996), "An experimental study of round jets in crossflow," *J. of Fluid Mech.*, 306, 111-144.
- Krothapalli, A., Baganoff, D., and Karamcheti, K. (1981), "On the mixing of a rectangular jet," *J. of Fluid Mech.*, 107, 201 - 220.
- Lauder, B.E. and Spalding, D.B. (1974), "The numerical computation of turbulent flows," *Comp. Math. Appl. Mech., Eng.*, Vol. 3, 269 - 289.
- Milovan, P. and Scheuerer, G. (1989), "CAST - a finite volume method for predicting two-dimensional flow and heat transfer phenomena," GRS-Technical Notiz SRR-89-01
- Ogino, F., Takeuchi, H., Kudo, I., and Mizushima, T. (1980), "Heated jet discharged vertically into ambient of uniform and linear temperature profiles," *Int. J. Heat Mass Transfer*, 23, 1581 - 2365.
- Patankar, S. V. (1980), "Numerical heat transfer and fluid flow," Hemisphere Publ. Corp., Washington.
- Raman, G. and Taghavi, R. (1996), "Resonant interaction of a linear array of supersonic rectangular jets: an experimental study," *J. of Fluid Mech.*, 309, 93 - 111.
- Roth, K. (1988), "Application of a three-dimensional Navier-Stokes model for a subsonic jet in a crossflow," Ph.D. thesis, Florida University.
- Rottman, W.T., Simpson, J.E. and Stansby, P.K. (1987), "The motion of a cylinder of fluid released from rest in a crossflow," *J. of Fluid Mech.*, 177, 307 - 337.
- Schetz, J. A. (1980), "Injection and mixing in turbulent flow," *Progress in Astronautics and Aeronautics*, Vol. 68.
- Smith, S.H. (1996), "The scalar concentration field of the axi-symmetric jet in crossflow," Ph.D. thesis, Stanford University.
- Smith, S.H. and Mungal, M.G. (1998), "Mixing, structure and scaling of the jet in crossflow," *J. of Fluid Mech.*, 357, 83 - 122.